



Assessment of Age-Related Morphological and Functional Changes of Selected Structures of the Head and Neck by Computed Tomography, Magnetic Resonance Imaging, and Positron Emission Tomography

Anton Mahne, MD, Ghassan El-Haddad, MD, Abass Alavi, MD, Mohamed Houseni, MD, Gul Moonis, MD, Andrew Mong, MD, Miguel Hernandez-Pampaloni, MD, PhD, and Drew A. Torigian, MD, MA

The head and neck is a complex anatomical region that can be evaluated using many imaging modalities. It is important to discern normal structures from ones that are affected by disease and to study how these structures change in their morphological and functional properties with aging. Therefore, using magnetic resonance imaging (MRI), we retrospectively evaluated volumes of the parotid glands, submandibular glands, thyroid gland, tongue, soft palate, and lingual tonsils in 64 subjects ages 13 to 81 years. Volume, attenuation (HU), and metabolic activity (maximum SUV) of the parotid, submandibular, and thyroid glands were assessed retrospectively using positron emission tomography/computed tomography (PET/CT) imaging in 35 subjects ages 10 to 76 years. Metabolic activity (maximum SUV) of the parotid, submandibular, and sublingual glands; tongue; adenoids; and tonsils (lingual and palatine) were evaluated retrospectively using PET imaging in 15 subjects ages 6 to 20 years. Metabolic volumetric products of the parotid, submandibular, and thyroid gland were calculated and analyzed with increasing age in subjects who underwent PET/CT imaging. Structures that exhibited statistically significant changes ($P < 0.05$) with increasing age included the submandibular glands, thyroid gland, soft palate, and adenoids. The CT volume of the submandibular glands increased with age, and the attenuation decreased with age with statistical significance. The thyroid gland volume, as measured using MRI, showed a statistically significant decrease with aging. The volume of the soft palate and lingual tonsils, as measured by MRI, exhibited a statistically significant decrease in volume with aging. The maximum SUV of the adenoids demonstrated a statistically significant decrease with aging. In conclusion, CT, MRI, and PET may be used to quantitatively and qualitatively assess structures of the head and neck and are useful in the assessment of structural and functional changes of these structures with aging. Semin Nucl Med 37:88-102 © 2007 Elsevier Inc. All rights reserved.

The head and neck is an intricate area of the human body in which numerous organ systems coexist. Many anatomic structures reside in this confined space, all of which are susceptible to a wide range of pathology. An understanding of how these structures change in the aging human is para-

mount for the differentiation of normal and pathological states. At times, it may be difficult to distinguish in the head/neck what is considered a "normal" process of aging from a pathological process of structures, although many imaging modalities can be used to evaluate subjects presenting with complaints referable to the head and neck region.

Structures of the head and neck, in particular the salivary glands, historically were evaluated using conventional plain film radiography and sialography. However, technological advancements, including magnetic resonance imaging (MRI), computed tomography (CT), and ^{18}F -fluorodeoxyglucose

Department of Radiology, University of Pennsylvania School of Medicine, Philadelphia, PA.

Address reprint requests to Drew A. Torigian, MD, MA, Department of Radiology, Hospital of the University of Pennsylvania, 3400 Spruce Street, Philadelphia, PA 19104-4283. E-mail: Drew.Torigian@uphs.upenn.edu

(FDG) positron emission tomography (PET), have revolutionized the way the head and neck are imaged. MRI has been reported to have superior soft-tissue contrast resolution and depicts lesions in the parotid gland more accurately than CT.¹ Technical improvements, multiplanar imaging capabilities, and increased clinical experience with MRI have favored its use relative to other imaging modalities for evaluation of the major salivary glands.²

Evaluation of the head and neck with FDG-PET is important for evaluation of primary head and neck malignancies and also for metastatic disease, systemic disease, infection, and inflammation. However, because of the relatively high physiologic uptake in complex structures of the pharynx and neck, interpretation of PET images of the head and neck can be challenging.³ With the advent of PET/CT, it has become easier and more reliable to localize radiotracer uptake to specific head and neck structures.

In this article, we will present our quantitative preliminary data regarding evaluation of age-related changes of structures in the head and neck region using CT, MRI, and PET. We will also review the literature and discuss previous studies relevant to this topic of interest. We believe that this will provide a better understanding of the changes in morphology and function of selected structures in the head and neck region with increasing age, and will provide a basis for future research in this area.

Materials and Methods

We obtained Institutional review board approval for retrospective data collection and image analysis along with a HIPAA waiver from the University of Pennsylvania's and the Children's Hospital of Philadelphia's Institutional Review Boards before the study's initiation.

Sixty-four subjects (25 male, 39 female) between the ages of 13 to 81 years old who had undergone an MRI of the head and neck region were evaluated retrospectively. All MRI examinations were performed on a 1.5-T magnet. Structures examined were the parotid glands, submandibular glands, thyroid gland, tongue, soft palate, and lingual tonsils. Subjects who did not have cancer, masses, or other known abnormalities in the head and neck region and who had normal MRI reports were selected for inclusion. Any subject with an abnormality of the head and neck region was excluded.

Axial T1-weighted images were obtained with a slice thickness (ST) of 5 mm and interval space (IS) ranging between 5 to 6.5 mm. Regions of interest were drawn manually along the boundaries of the parotid glands, submandibular glands, and thyroid lobes bilaterally on multiple axial slices through each structure, beginning at the most superior border where the structure was visualized and continuing inferiorly to the most inferior border; then, area values were recorded. Area measurements of the lingual tonsils were obtained on axial T2-weighted images with a ST of 5 mm and IS of 5 to 5.5 mm. Regions of interest were drawn manually using the same technique as described previously, and area measurements were recorded. Area measurements of the tongue and soft palate

were obtained on sagittal T1-weighted images with a ST of 5 mm and IS 6 to 6.6 mm. Regions of interest along the boundaries of these structures were drawn manually, beginning at one lateral border and ending where the structure of interest was no longer visualized; then, area measurements were recorded. Recorded cross-sectional areas were then multiplied by IS values to obtain structure volumes in cm³.

We then retrospectively reviewed whole-body PET/CT scans (Gemini TF; Philips Medical Systems, Bothell, WA) of 35 subjects (19 male, 16 female; age range, 10-76 years), who had been referred to our PET center mainly for oncologic indications. Subjects fasted for at least 4 hours before imaging, and serum glucose levels were <140 mg/dL in all subjects. CT scan images were obtained using a low-dose protocol (50-150 mAs) with a 5-mm ST. PET was initiated 60 minutes after the intravenous administration of a dose of ¹⁸F-FDG adjusted to the body weight (215 μ Ci/kg (7.9 MBq/kg)). Subsequently, 3D PET data were acquired using 3-minute table positions. The PET acquisition included a time-of-flight and a dead-time correction as well as online delayed coincidence subtraction to correct for random coincidences. Rescaled CT images were used to produce attenuation correction values for the PET emission reconstruction. Subjects were selected who did not have cancer, masses, or other known abnormalities in the head and neck region. Subjects with thyroid goiter were excluded from analyses pertaining to the thyroid gland.

If subjects had a history of cancer outside of the head and neck, they were selected according to the following criteria: (1) no known history of head and neck metastatic lesions, (2) no chemotherapy at least 3 months before the study, (3) no prior radiation therapy to the head and neck region, (4) no past surgical history involving the head and neck region, and (5) no other abnormalities in the head and neck region. Structures evaluated included the parotid, submandibular, and thyroid glands. Regions of interest were traced manually about the margins of the structures bilaterally on axial images, beginning at the most superior border and continuing inferiorly to the most inferior border; then, area values were recorded. Maximum standardized uptake values (SUV), attenuation values in Hounsfield units (HU), and volumes (cm³) were then calculated using the Syntegra computer program (Philips Medical Systems, v. 2.1F). Metabolic volumetric products (MVPs), defined as the maximum SUV multiplied by the structure volume (in units of SUV-cm³), also were calculated for the parotid, submandibular, and thyroid gland with increasing age.

A retrospective analysis also was performed on 15 subjects (11 male, 4 female; age range, 6-20 years) who had dedicated whole-body PET scans (Allegro; Philips Medical Systems or C-PET; ADAC UGM Medical Systems, Milpitas, CA) for oncologic indications. Subjects selected followed the same inclusion and exclusion criteria as described previously for the PET/CT group. The subjects fasted for at least 4 hours, and serum glucose levels were <140 mg/dL in all subjects. No specific preparation was given to the subjects. PET was initiated 60 minutes after

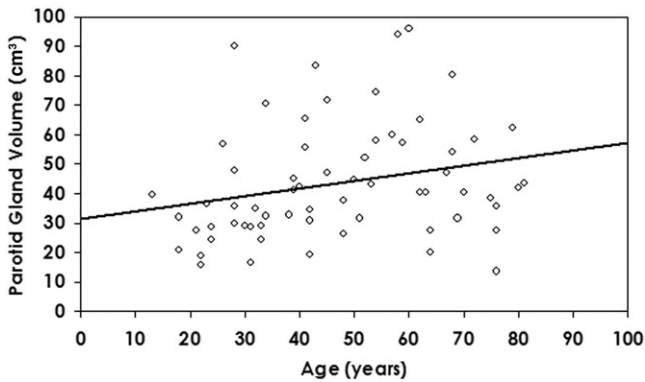


Figure 1 Changes in parotid gland volume on MRI with age ($r = 0.24$, $P = 0.06$).

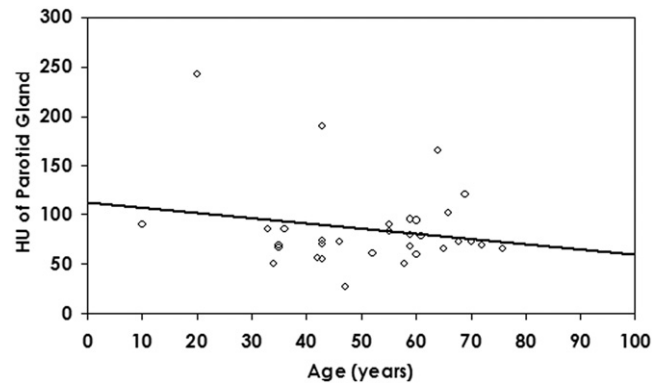


Figure 3 Changes in attenuation (HU) of parotid glands with age ($r = -0.3$, $P = 0.1$).

the intravenous administration of a dose of ^{18}F -FDG adjusted to the body weight ($140 \mu\text{Ci}/\text{kg}$ ($5.2 \text{ MBq}/\text{kg}$) for the Allegro and $50 \mu\text{Ci}/\text{kg}$ ($1.9 \text{ MBq}/\text{kg}$) for the C-PET ADAC camera. Transmission scans obtained with a ^{137}Cs point source were interleaved between the multiple emission scans to correct for nonuniform attenuation. Axial images of the parotid, submandibular and sublingual glands, tongue, adenoids, and tonsils (lingual and palatine) were evaluated. Regions of interest were drawn manually around visible portions of these structures, beginning superiorly and continuing inferiorly until the activity was no longer visualized. Maximum SUVs were calculated from these regions of interest and recorded for each subject.

Calculated volumes, attenuation values, and maximum SUVs from structures with bilateral representation were each added together and averaged to give the final values. All scatterplots were performed with Microsoft Excel software (Microsoft Corporation; Redmond, WA). For statistical analysis, Pearson correlation coefficients were calculated between volume, maximum SUV, and attenuation with increasing age as described below. For all measurements, $P < 0.05$ was considered to be statistically significant. All statistical analyses were performed using SPSS version 14.0 (SPSS Inc, Chicago, IL).

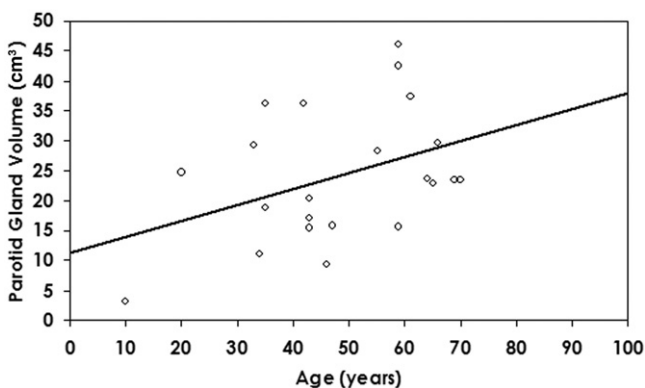


Figure 2 Changes in parotid gland volume on PET/CT with age ($r = 0.2$, $P = 0.3$).

Results

Parotid Glands

The volumetric analysis performed using MRI demonstrated a nonsignificant increase in parotid gland volume with increasing age ($r = 0.24$, $P = 0.06$; Fig. 1). The volume of the parotid glands in a separate population, as measured using PET/CT imaging, also showed a nonsignificant increase in volume with increasing age ($r = 0.2$, $P = 0.3$; Fig. 2). The attenuation of the parotid glands was found to exhibit a nonsignificant decrease with increasing age ($r = -0.3$, $P = 0.1$; Fig. 3). The average maximum attenuation in males was found to be 85 HU (SD 44), whereas for females it was 82 HU (SD 34), exhibiting a nonsignificant difference between genders ($P = 0.8$).

The relationship between parotid gland volume and gender also was evaluated. The mean parotid gland volume as measured by MRI for males was found to be 55 cm^3 (SD, 19; range, 20-96 cm^3), whereas for females it was 36 cm^3 (SD, 16; range, 13-72 cm^3), demonstrating a significant difference between genders ($P < 0.0001$). The mean parotid gland volume as measured by CT for males was found to be 25 cm^3 (SD, 12; range, 3-42 cm^3), whereas for females it was 17 cm^3 (SD, 9; range, 11-36 cm^3), demonstrating a nonsignificant difference between genders ($P = 0.15$).

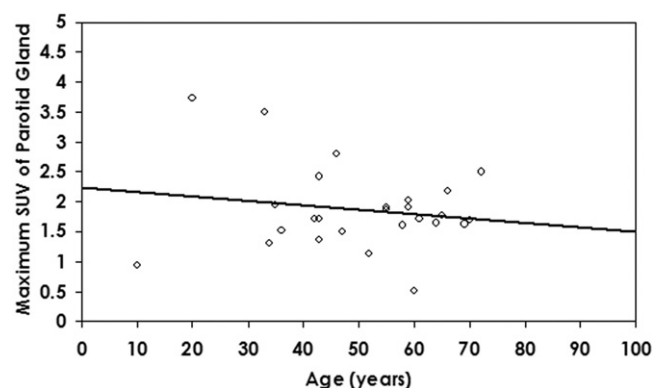


Figure 4 Changes in maximum SUV of parotid glands with age ($r = -0.17$, $P = 0.42$).

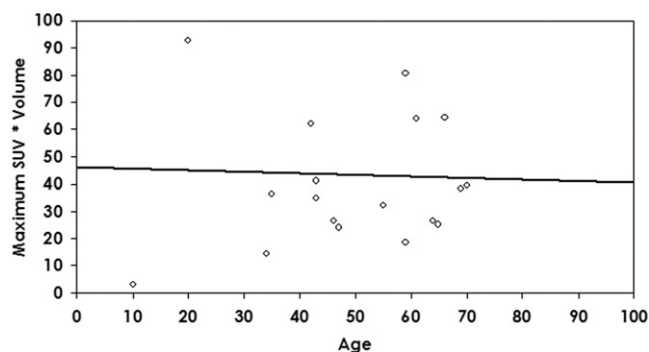


Figure 5 Changes in MVP of parotid glands (units of SUV-cm³) on PET-CT with age ($r = -0.03$, $P = 0.9$).

The relationship between right and left parotid gland volume across both genders also was evaluated. In our MRI group, there was no significant difference between right and left parotid gland volume ($P = 0.8$). The average volume of the right parotid gland was 4.2 cm³ (SD, 2) and the left was 4.2 cm³ (SD, 1.8). In our PET/CT group, there was no significant difference between right and left parotid gland volume ($P = 0.9$). The average volume of the right parotid gland was 9.9 cm³ (SD 6) and that of the left was 9.9 cm³ (SD 6).

The maximum SUV of the parotid glands in our PET/CT group of subjects showed a nonsignificant decrease with increasing age ($r = -0.17$, $P = 0.42$; Fig. 4). The average maximum parotid gland SUV in males was 2.1 (SD, 0.7), whereas for females it was 1.6 (SD, 0.5), demonstrating a nonsignificant difference between genders ($P = 0.1$).

MVPs for the parotid gland in this PET/CT group demonstrated no significant change with increasing age ($r = -0.03$, $P = 0.9$; Fig 5). The relationship between right and left parotid gland activity (maximum SUV) across both genders was also evaluated. In our PET/CT group, there was no significant difference between right and left parotid gland activity ($P = 0.2$). The average maximum SUV of the right parotid gland was 2.0 (SD, 0.9) and that of the left was 1.7 (SD, 0.6).

Dedicated PET scans of our pediatric population suggested a nonsignificant increase in the maximum SUV of the parotid glands with increasing age ($r = 0.32$, $P = 0.3$; Fig. 6). The average maximum SUV in males was found to be 1.5 (SD,

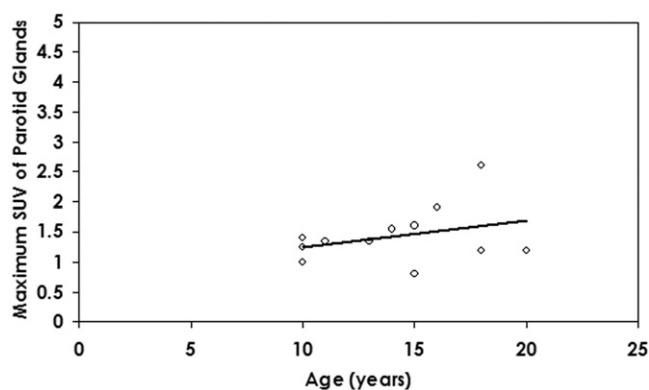


Figure 6 Changes in maximum SUV of parotid glands with age ($r = 0.32$, $P = 0.3$).

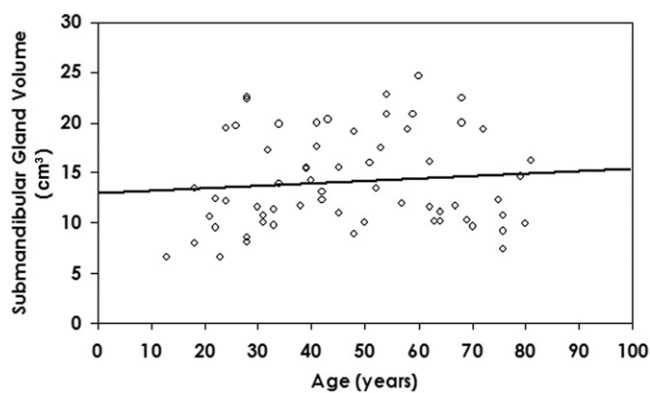


Figure 7 Changes in submandibular gland volume on MRI with age ($r = 0.1$, $P = 0.5$).

0.5), whereas for females it was 1.2 (SD, 0.3), demonstrating a nonsignificant difference between genders ($P = 0.3$).

Submandibular Glands

The volumetric analysis performed using MRI demonstrated no significant change in submandibular gland volume with increasing age ($r = 0.1$, $P = 0.5$; Fig. 7). We noted that the volume of the submandibular glands in a separate population, as measured using PET/CT imaging, was significantly positively correlated with increasing age ($r = 0.5$, $P < 0.05$; Fig. 8). The attenuation of the submandibular glands was found to exhibit a significant negative correlation with increasing age ($r = -0.37$, $P < 0.05$; Fig. 9). The average maximum attenuation for males was found to be 96 HU (SD 22), whereas for females it was 83 HU (SD 23), demonstrating a nonsignificant difference between genders ($P = 0.1$).

The relationship between submandibular gland volume and gender also was evaluated. The mean submandibular gland volume as measured by MRI for males was found to be 16.5 cm³ (SD, 5; range, 6-25 cm³), whereas for females it was 12.6 cm³ (SD, 3; range, 6-19 cm³), demonstrating a significant difference between genders ($P < 0.01$). The mean submandibular gland volume as measured by CT for males was found to be 11.1 cm³ (SD, 5; range, 7-20 cm³), whereas for females it was 12.2 cm³ (SD, 5; range, 5-23 cm³), dem-

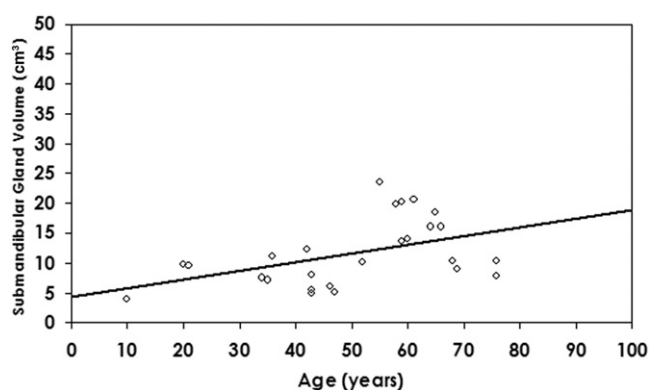


Figure 8 Changes in submandibular gland volume on PET-CT with age ($r = 0.5$, $P < 0.05$).

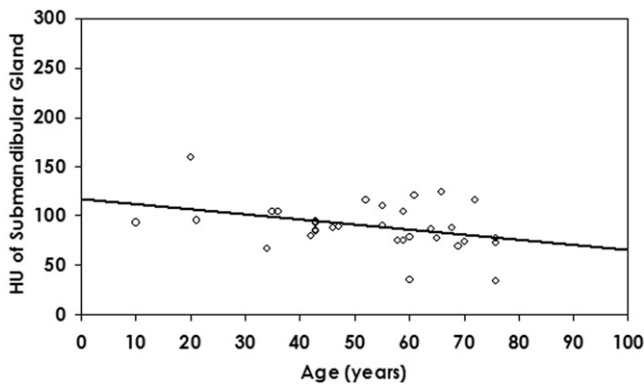


Figure 9 Changes in attenuation (HU) of submandibular glands with age ($r = -0.37, P < 0.05$).

onstrating a nonsignificant difference between genders ($P = 0.6$).

The relationship between right and left submandibular gland volume across both genders also was evaluated. In our MRI group, there was no significant difference between right and left submandibular gland volume ($P = 0.9$). The average volume of the right submandibular gland was 1.4 cm^3 (SD, 0.5) and the left was 1.4 cm^3 (SD, 0.5). In our PET/CT group, there was no significant difference between right and left submandibular gland volume ($P = 0.8$). The average volume of the right submandibular gland was 6.1 cm^3 (SD, 3.1) and that of the left was 5.9 cm^3 (SD, 2.7).

The maximum SUV of the submandibular glands in our group of subjects showed a nonsignificant decrease with increasing age ($r = -0.22, P = 0.3$; Fig. 10). The average maximum submandibular gland SUV in males was 2.5 (SD, 0.5), whereas for females it was 2.1 (SD, 0.9), demonstrating a nonsignificant difference between genders ($P = 0.2$). MVPs for the submandibular gland in this PET/CT group demonstrated a nonsignificant increase with increasing age ($r = 0.36, P = 0.09$; Fig. 11).

The relationship between right and left submandibular gland activity (maximum SUV) across both genders also was evaluated. In our PET-CT group, there was no significant difference between right and left submandibular gland activity ($P = 0.9$). The average maximum SUV of the right sub-

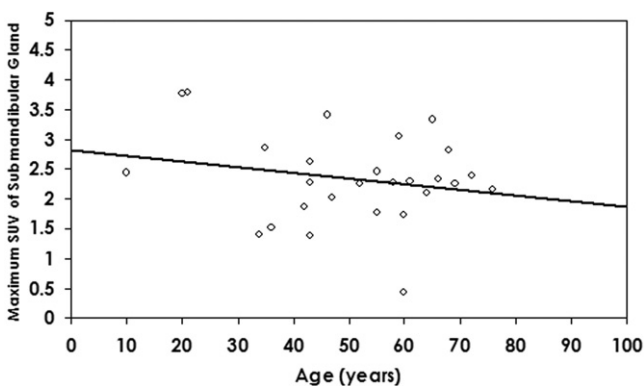


Figure 10 Changes in maximum SUV of submandibular glands with age ($r = -0.22, P = 0.3$).

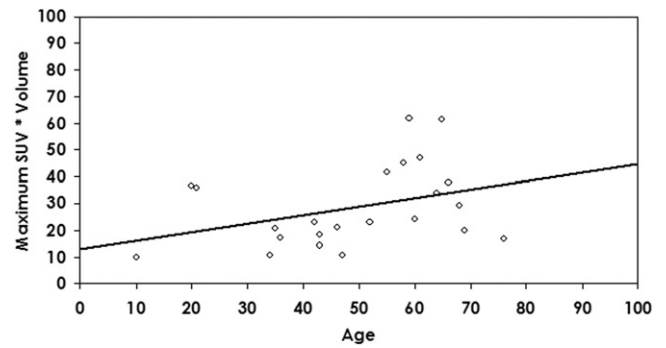


Figure 11 Changes in MVP of submandibular glands (units of SUV- cm^3) on PET/CT with age ($r = 0.36, P = 0.09$).

mandibular gland was 2.4 (SD, 0.6) and that of the left was 2.4 (SD, 0.8).

Dedicated PET scans of our pediatric population suggest a nonsignificant increase in maximum SUV of the submandibular glands with increasing age ($r = 0.36, P = 0.34$; Fig. 12). The average maximum SUV in males was 1.9 (SD, 0.7), whereas for females it was also found to be 1.9 (SD, 0.1), demonstrating a nonsignificant difference between genders ($P = 0.99$).

Thyroid Gland

The volumetric analysis performed using MRI showed a significant negative correlation between thyroid gland volume and increasing age ($r = -0.38, P < 0.05$; Fig. 13). The volume of the thyroid gland in a separate population, as measured using PET-CT imaging, did not demonstrate a significant change with increasing age ($r = -0.09, P = 0.6$; Fig. 14). The attenuation of the thyroid gland did not demonstrate a significant change with increasing age ($r = 0.02, P = 0.9$; Fig. 15). The average maximum attenuation for males was found to be 168 HU (SD, 41), whereas for females it was 153 HU (SD, 34), demonstrating a nonsignificant difference between genders ($P = 0.3$).

The relationship between thyroid gland volume and gender also was evaluated. The mean thyroid gland volume as measured by MRI for males was found to be 9.2 cm^3 (SD, 1.9; range, 5-14 cm^3), whereas for females it was 7.6 cm^3 (SD, 2.8;

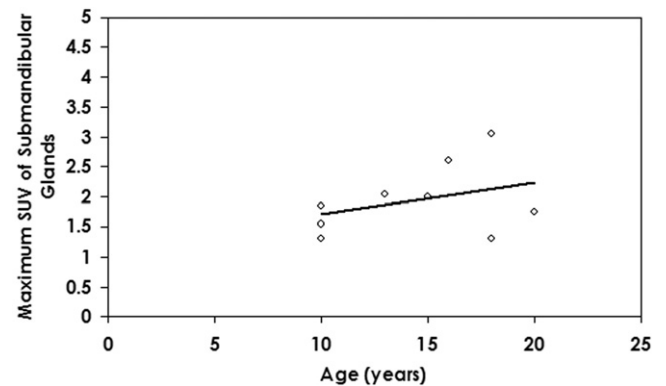


Figure 12 Changes in maximum SUV of submandibular glands with age ($r = 0.36, P = 0.34$).

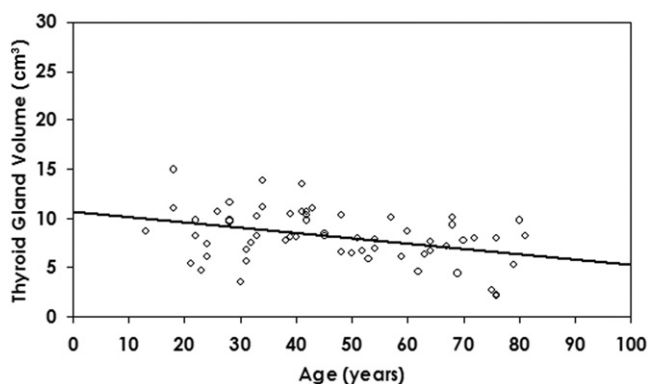


Figure 13 Changes in thyroid gland volume on MRI with age ($r = -0.38$, $P < 0.05$).

range, 2-15 cm³), demonstrating a significant difference between genders ($P < 0.01$). The mean thyroid gland volume as measured by CT for males was found to be 8.7 cm³ (SD, 2.8; range, 2-13 cm³), whereas for females it was 9.5 cm³ (SD, 3; range, 4-15 cm³), demonstrating a nonsignificant difference between genders ($P = 0.5$).

The relationship between right and left thyroid lobe volume across both genders was also evaluated. In our MRI group, there was no significant difference between right and left thyroid lobe volume ($P = 0.1$). The average volume of the right thyroid lobe was 0.9 cm³ (SD 0.3) and that of the left was 0.8 cm³ (SD 0.3).

The maximum SUV of the thyroid gland in our PET-CT group of subjects showed that there was no significant change with increasing age ($r = 0.03$, $P = 0.9$; Fig. 16). The males in our study had an average maximum SUV of 1.8 (SD 0.7), whereas for females it was 1.9 (SD 0.6), demonstrating a nonsignificant difference between genders ($P = 0.7$). MVPs for the thyroid gland in this PET/CT group demonstrated no significant change with increasing age ($r = -0.03$, $P = 0.9$; Fig. 17).

Tongue, Soft Palate, Lingual and Palatine Tonsils, Adenoids, and Sublingual Glands

Volumetric analysis of the tongue, soft palate, and lingual tonsils were performed by measurements from MRI exam-

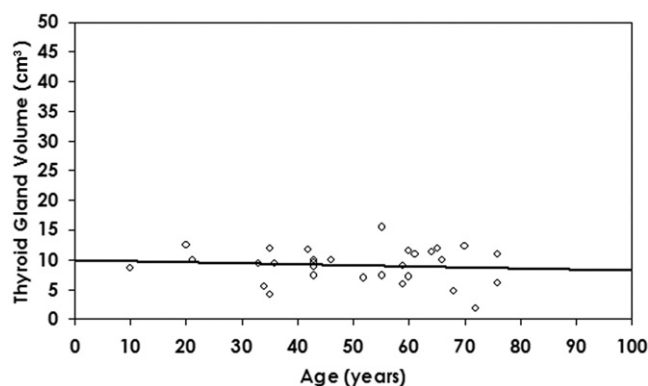


Figure 14 Changes in thyroid gland volume on PET-CT with age ($r = -0.09$, $P = 0.6$).

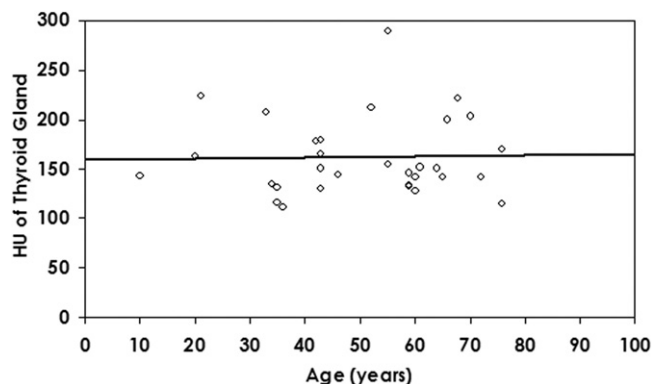


Figure 15 Changes in attenuation (HU) of thyroid gland with age ($r = 0.02$, $P = 0.9$).

inations of the head and neck. The volume of the tongue showed no significant change with increasing age ($r = -0.04$, $P = 0.7$; Fig. 18). The average tongue volume for males was 64.6 cm³ (SD, 8.8; range, 51-88 cm³), whereas for females it was 51.2 cm³ (SD, 8.8; range, 36-80 cm³), demonstrating a significant difference between genders ($P < 0.00001$).

We were unable to accurately calculate the volume and maximum SUV of the tongue in our PET/CT subjects because of the presence of beam hardening artifacts related to dental amalgam. In our pediatric population studied by PET alone, there was a nonsignificant increase in the maximum SUV of the tongue with increasing age ($r = 0.4$, $P = 0.19$; Fig. 19). The average maximum SUV for males was 1.6 (SD 0.4), whereas for females it was 1.5 (0.2), demonstrating a nonsignificant difference between genders ($P = 0.7$).

The soft palate showed a significant negative correlation between volume and increasing age ($r = -0.4$, $P < 0.05$; Fig. 20). The mean soft palate volume in males evaluated by MRI was found to be 2.4 cm³ (SD, 0.7; range, 1.3-4.1 cm³), whereas for females it was 1.8 cm³ (SD, 0.7; range, 0.9-3.5 cm³), demonstrating a nonsignificant difference between genders ($P = 0.09$).

The lingual tonsils demonstrated a significant negative correlation between volume and increasing age ($r = -0.67$; $P < 0.05$; Fig. 21). The average volume of the lingual tonsils

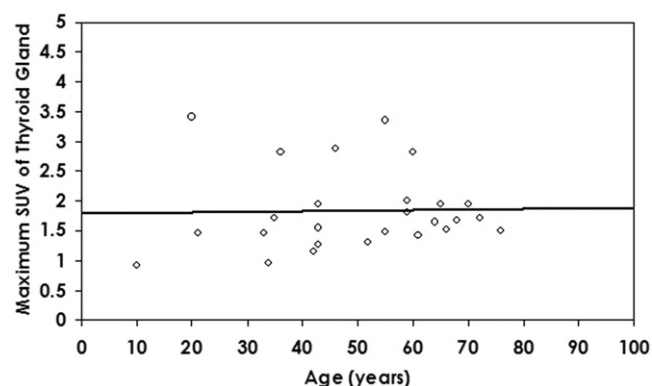


Figure 16 Changes in maximum SUV of thyroid gland with age ($r = 0.03$, $P = 0.9$).

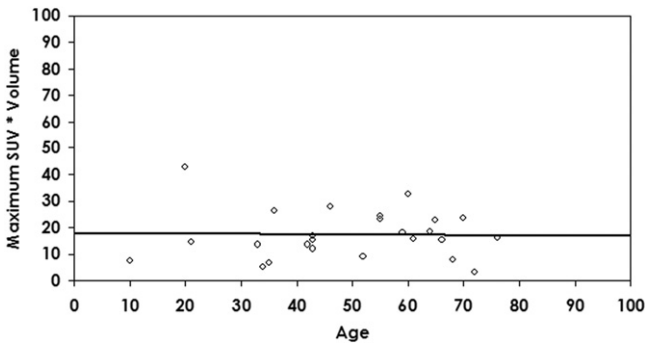


Figure 17 Changes in MVP of thyroid gland (units of SUV-cm³) on PET-CT with age ($r = -0.03, P = 0.9$).

evaluated by MRI in males was found to be 4.1 cm³ (SD, 2.6; range, 0.5-9.2 cm³), whereas for females it was 2.5 cm³ (SD, 1.4; range, 0.5-4.9 cm³), demonstrating a nonsignificant difference between genders ($P = 0.02$).

The relationship between right and left lingual tonsil volumes across both genders was also evaluated. In our MRI group, there was no significant difference between right and left lingual tonsil volume ($P = 0.8$). The average volume of the right lingual tonsil was 0.2 cm³ (SD 0.2) and that of the left was 0.2 cm³ (SD 0.2).

We were unable to accurately calculate the maximum SUV of the lingual tonsils in our PET-CT subjects due to the presence of beam hardening artifacts due to dental amalgam. In our pediatric population, the maximum SUV of the lingual tonsils exhibited a nonsignificant increase with increasing age ($r = 0.3, P = 0.4$; Fig. 22), whereas the maximum SUV of the palatine tonsils exhibited no significant change with increasing age ($r = -0.02, P = 0.9$; Fig. 23). The maximum SUV of the lingual tonsils in males was found to be 3.1 (SD, 1), whereas for females it was 3.5 (SD, 1.2), demonstrating a nonsignificant difference between genders ($P = 0.6$). The maximum SUV of the palatine tonsils in males was 3.1 (SD, 0.6), whereas for females it was 2.4 (0.6), demonstrating a nonsignificant difference between genders ($P = 0.1$).

The maximum SUV of the adenoids in our pediatric population was found to exhibit a significant negative correlation with increasing age ($r = -0.8, P < 0.05$; Fig. 24). The

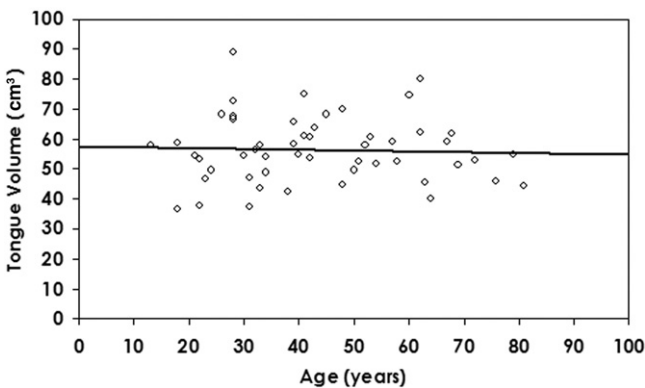


Figure 18 Changes in tongue volume on MRI with age ($r = -0.04, P = 0.7$).

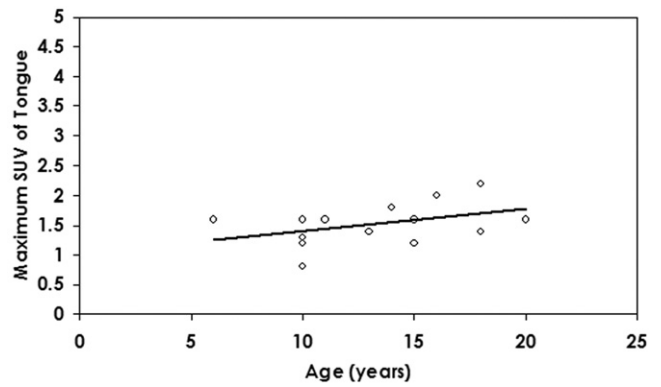


Figure 19 Changes in maximum SUV of tongue with age ($r = 0.4, P = 0.15$).

average maximum SUV for males was 3.5 (SD 0.4). We were not able to calculate the average maximum SUV in females due to a small sample size.

We were unable to accurately calculate the maximum SUV of the sublingual glands in our PET-CT subjects due to beam hardening artifacts related to dental amalgam. The maximum SUV of the sublingual glands in our pediatric population demonstrated a nonsignificant increase with increasing age ($r = 0.44, P = 0.13$; Fig. 25). The average maximum SUV for males was 2.5 (SD, 0.9), whereas for females it was 2.0 (SD, 0.4), demonstrating a nonsignificant difference between genders ($P = 0.4$).

Discussion

Salivary Glands

Embryologically, the parotid glands are the first salivary glands to develop, followed by the submandibular glands, and then the sublingual glands. The parotid gland becomes encapsulated late in the second trimester after the submandibular and sublingual glands, and before the parotid gland encapsulates, the lymphatic system begins to emerge in the mesoderm. Hence, in the adult, there are intraglandular lymph nodes and lymphatic tissue within the parotid glands but not in the remaining salivary glands.^{4,5}

CT and MRI can successfully identify the parotid gland

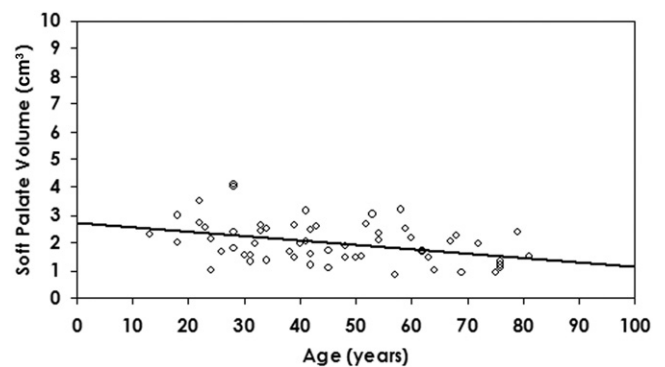


Figure 20 Changes in soft palate volume on MRI with age ($r = -0.4, P < 0.05$).

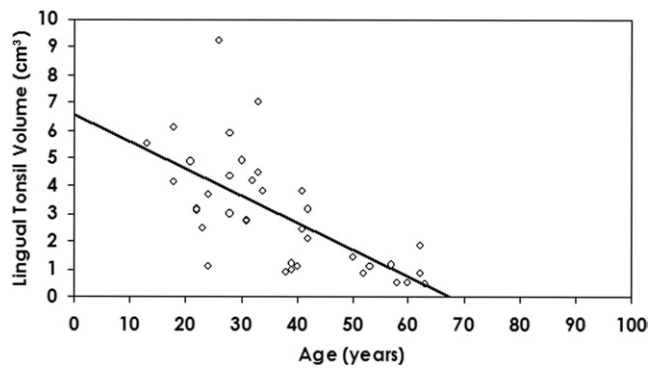


Figure 21 Changes in lingual tonsil volume on MRI with age ($r = -0.67$, $P < 0.05$).

and show changes that occur with development and again, as well as with the development of pathology.¹ The parotid gland is divided into superficial and deep lobes by the plane of the facial nerve and is bordered by the masseter muscle anteriorly, the pterygoid muscles medially, as well as by the styloid process, carotid arteries, jugular vein, and parapharyngeal space. Variations in normal anatomy of the parotid gland are important to be aware of. Medbery and coworkers made the following observations regarding normal variation in parotid location: (1) parotid glands can extend anterior to the masseter muscle or posterior to the posterior margin of this muscle; (2) parotid glandular tissue can extend above the zygoma and external auditory canal; (3) parotid tissue can extend posteriorly to overlap the vertebra; (4) parotid glands can extend below or remain above the angle of the mandible; and (5) parotid glands can widely vary in transverse dimension.⁶ A normal salivary gland in an abnormal position may potentially be mistaken for a pathological lesion on a CT or MRI scan and also can lead to a misdiagnosis of malignancy on PET imaging.

Scott and coworkers have shown in a postmortem study of the parotid glands that acinar atrophy and ductal irregularities correlate with advancing age. In the same study, adipose tissue together with fibrovascular tissue tended to increase with age, and there was a 30% reduction in acinar volume.⁷ Dong and coworkers studied the morphologic changes in the

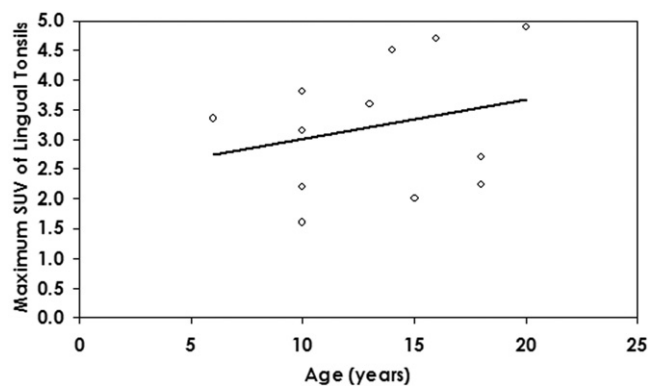


Figure 22 Changes in maximum SUV of lingual tonsils with age ($r = 0.3$, $P = 0.4$).

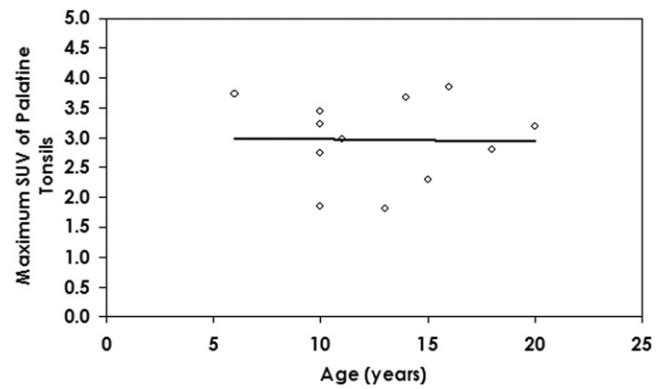


Figure 23 Changes in maximum SUV of palatine tonsils with age ($r = -0.02$, $P = 0.9$).

histologic structure of human submandibular glands sampled during surgery and showed that the volume of parenchymal cells in the elderly population decreased by 23% compared with that of the younger population, with a 31.2% decrease in volume of acinar tissue and an increase of fat and fibrous tissue by 2-fold and 0.8-fold, respectively.⁸ Kurashima and coworkers have shown that the presence of focal lymphocytic infiltration in postmortem submandibular glands was seen more frequently in patients older than 70 years of age (80.3%), compared with those younger than 70 (53.8%).⁹ Another postmortem study by Azevedo and coworkers found that, with increasing age, the sublingual glands underwent acinar atrophy, ductal irregularities, and parenchymal replacement by fibrous and/or adipose tissue.¹⁰ Age-induced variations and reactive changes in the major salivary glands include oncocyte proliferation, fatty infiltration, squamous and mucous metaplasia, hyperplasia, atrophy, and regeneration.¹¹ Dayan and coworkers have demonstrated that there is a 48% decrease in mean acinar volume from biopsies of palatal salivary glands between the young and old groups, along with significant age-related increases in intercalated ducts, blood and lymphatic vessels, adipose tissue, and connective tissue.¹² Not only can the salivary glands become infiltrated with adipose tissue, but so may the surrounding connective tissue, which may be independent of the overall body habitus.¹³

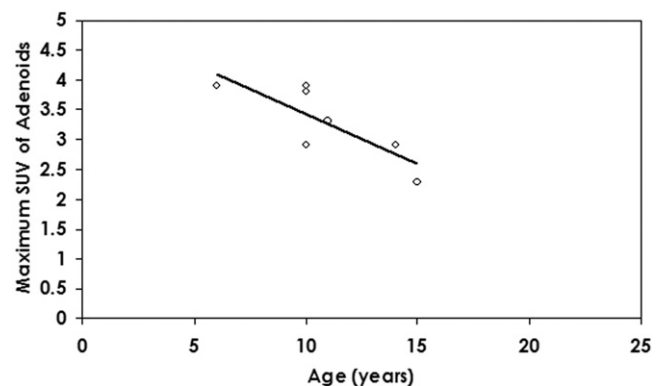


Figure 24 Changes in maximum SUV of adenoids with age ($r = -0.8$, $P < 0.05$).

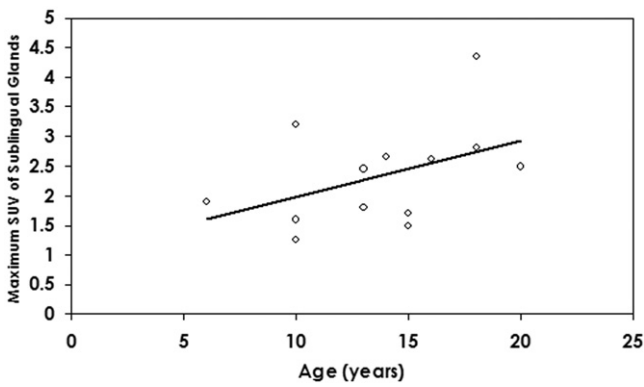


Figure 25 Changes in maximum SUV of sublingual glands with age ($r = 0.44$, $P = 0.13$).

Sumi and coworkers found that the T1-weighted signal intensity of the parotid glands increased with age, although the signal intensity of the sublingual and submandibular glands did not, and postulated that the cause of the discrepancies in signal intensity between the three major salivary glands were related to differences in content of adipose tissue. This was supported by the finding that the parotid gland attenuation has an age-related decrease on CT, indicating an increased adipose component in the parenchyma.¹⁴ However, some CT studies of the parotid and submandibular glands have shown that the attenuation of both glands decrease with age, which is thought to be related to a decrease in mean acinar volume and an increase in fibrofatty tissue within the major salivary glands.¹⁵⁻¹⁹ In one study, Heo and coworkers performed quantitative analysis of the submandibular glands by calculating the maximum cross-sectional area on CT and showed a decrease in the size of the submandibular glands with age in a Korean population.¹⁸ Yonetsu and coworkers found a similar relationship in a Japanese population.¹⁹ Sumi and coworkers used quantitative MRI to show that the size of the sublingual glands decreased gradually with age.¹⁴

In our study, we have found that the attenuation of the parotid and submandibular glands showed a tendency to decrease with increasing age, in keeping with the reported histopathologic changes in those glands described above that occur with aging.⁷⁻¹⁴ Furthermore, volumes of the parotid glands were seen to increase with age, and volumes of the

submandibular glands either remained stable or increased with age based on MRI or CT measurements, respectively.

Previous studies have evaluated the function of the salivary glands, suggesting that there are age-related alterations in salivary function, including a significant age-related decrease in secretion rates.²⁰ It has been postulated that salivary gland dysfunction is a normal part of the aging process.²¹ In contrast, other studies have evaluated salivary flow rates and have concluded that major salivary gland output is age-stable, suggesting that salivary gland dysfunction (xerostomia) in an older person should not be considered a normal process of aging.^{22,23} More recently, other studies also have suggested that there is no direct age effect on salivary flow rates measured under different conditions of stimulation.²⁴ Furthermore, several investigators have evaluated the concept of secretory reserve capacity, whereby even though there is a loss of acinar cells in major salivary glands, saliva production remains age stable.^{25,26} It is thought that younger people have an excess of acini and, as they age, they lose a certain amount of acinar volume. Function is not compromised under normal conditions with increasing age because there is an excess amount of acini present early on. However, because the number of acini decreases with age, the gland may have a decrease in function with stress, such as that induced by the anticholinergic glycopyrrolate.²⁶

Stahl and coworkers evaluated the excretion of FDG into saliva and its significance on PET imaging, and have suggested that the increased uptake identified in the floor of the mouth was not from the sublingual glands but was within muscles. They concluded that the sublingual glands should be expected to behave similarly to the other major salivary glands, and that the muscles of the floor of the mouth involved in swallowing could not be totally controlled after FDG administration. They also concluded that the FDG concentration in saliva did not influence PET imaging, as tubes of saliva containing FDG placed beside the patient's neck during scanning were not visualized on PET imaging. They also showed that SUV measurements obtained before and after the patient drank water did not influence the radiotracer distribution in the head and neck.²⁷

Nakamoto and coworkers reported that FDG accumulation was variable in the normal parotid gland (mean SUV of 1.90; Fig. 26), submandibular gland (mean SUV of 2.11; Fig. 27), and

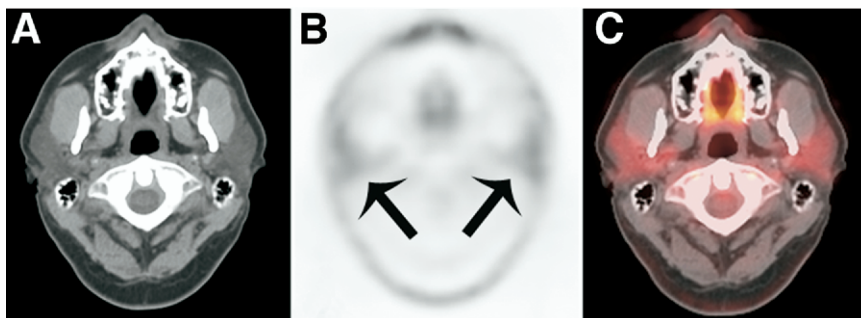


Figure 26 Axial images of a 42-year-old man demonstrating parotid glands (arrows) on CT (A), FDG-PET (B), and PET/CT (C). FDG uptake is noted in parotid glands (arrows) on PET (B) and PET/CT (C).

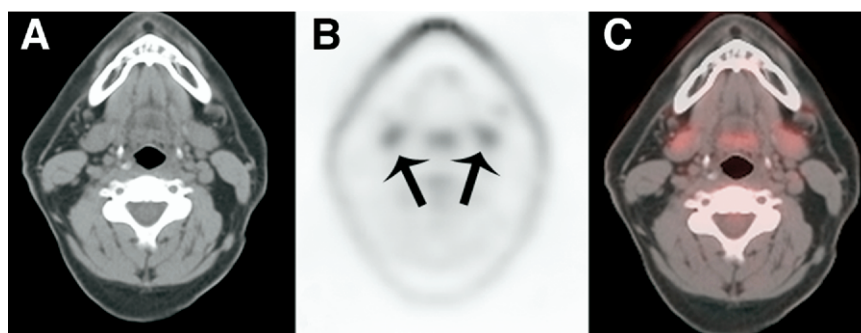


Figure 27 Axial images of a 35-year-old man demonstrating submandibular glands (arrows) on CT (A), FDG-PET (B), and PET/CT (C). FDG uptake is noted in submandibular glands (arrows) on PET (B) and PET/CT (C).

sublingual gland (mean SUV of 2.93; Fig. 28), with a negative correlation between age and physiologic FDG uptake in the sublingual glands on PET/CT.²⁸ Our results showed that maximum SUVs of the parotid and submandibular glands showed a tendency to decrease with increasing age, in keeping with acinar atrophy and that maximum SUVs of the parotid, submandibular, and sublingual glands had a tendency to increase in pediatric subjects. In our PET-CT subjects, the MVP of the parotid gland demonstrated no significant change with increasing age, while that of the submandibular gland demonstrated a nonsignificant tendency to increase with age.

Thyroid Gland

The thyroid gland is derived from the embryological foregut, is an important endocrine structure in the neck, and is located anterior to the trachea. When the volume of the thyroid gland is assessed, one must consider the gender of the subject because the thyroid gland is somewhat heavier in women and may become enlarged during menstruation or pregnancy.²⁹

Palpation of the thyroid gland to determine its size carries an inaccuracy rate of approximately 40%.³⁰ Ultrasonography has been used to evaluate the volume of the thyroid gland but may fail to completely measure enlarged thyroid glands that have substernal extension.³⁰ CT scanning has been used to quantify the volume of the thyroid gland in subjects with enlarged thyroids that have extended substernally and is an

easy, reliable, and reproducible method of determining thyroid gland volume.³¹ In determining the volume of the thyroid gland on CT, investigators reported that it is possible to calculate the thyroid volume by multiplication of the area obtained from manually traced regions of interest on axial slices by the interval thickness.^{31,32} We therefore used a similar method in our study to calculate thyroid gland volumes.

Hermans and coworkers evaluated thyroid gland volumes using CT and calculated postoperative thyroid gland weights in subjects with goiter. The average calculated thyroid volume by CT was 267 cm³, and the average postoperative thyroid gland weight was 243 g, with a mean difference between volume and weight of +12% ($r = 0.98$, $P < 0.001$) assuming that 1 cm³ of volume should equal 1 g of tissue, suggesting that CT overestimates the thyroid gland volume, possibly because of a distortion of adjacent fat planes and inclusion of nonthyroidal structures in areas of measurement. However, surgical intervention may also have decreased the true weight of the thyroid gland as a result of fluctuations in intraglandular fluid and blood volume or as the result of subtotal thyroidectomy, particularly because 50% of the subjects studied had substernal extension of the thyroid gland.³¹

The thyroid gland has variable uptake of FDG (Fig. 29).³ Moderate-to-intense uptake may be seen in the normal thyroid gland, although it may also be seen with thyroid inflammation, Graves' disease, or malignancy if focal.³³⁻³⁵ However,

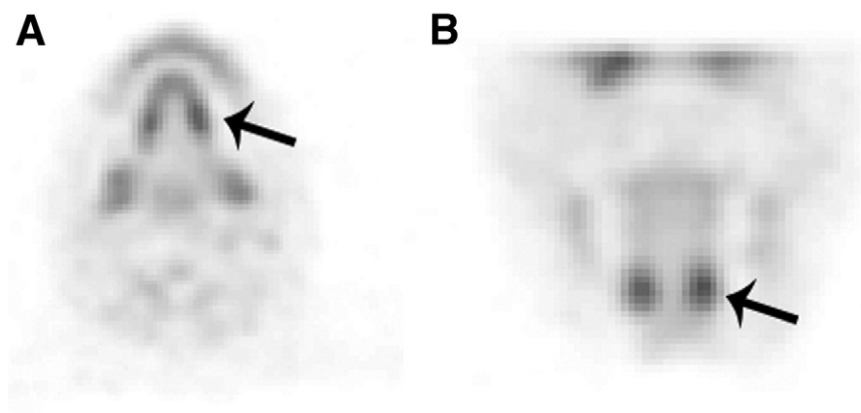


Figure 28 Axial (A) and coronal (B) PET images demonstrate FDG uptake in sublingual salivary glands (arrows) of a 17-year-old boy.

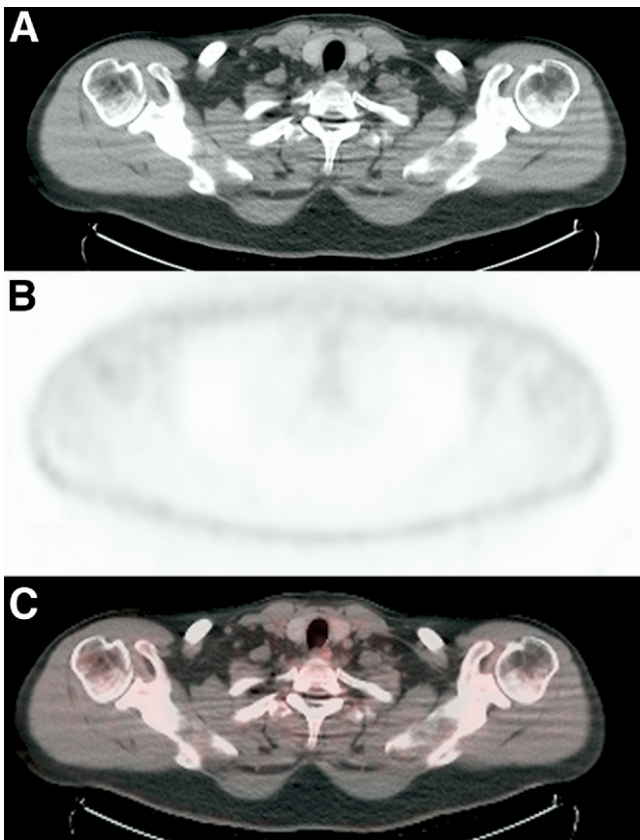


Figure 29 Axial images of a 58-year-old woman demonstrating thyroid gland on CT (A), FDG-PET (B), and PET/CT (C). Note minimal FDG uptake in thyroid gland of this particular subject.

Nakamoto and coworkers reported that minimal FDG uptake is seen in the normal thyroid gland (mean SUV of 1.31), and that mean thyroid SUV is slightly greater in men than in women on PET/CT.²⁸ PET/CT is superior to scintigraphic imaging alone to distinguish thyroid activity from activity in adjacent structures. Yi and coworkers evaluated the thyroid glands of 140 patients with newly diagnosed nonsmall cell lung cancer and found that on PET/CT images, thyroid FDG uptake was not likely to be misinterpreted as adjacent nodal uptake, and that there was less of a tendency to disregard increased FDG activity as representing normal variation when a corresponding morphologic abnormality is seen.³⁶

A study by Dvorakova and coworkers suggested that thyroid gland volume increases with age based on ultrasonographic measurement. Their study involved subjects ages 18 to 65 years from areas of known moderate iodine deficiency in the Czech Republic.³⁷ However, a study by Brown and coworkers evaluated the volume and histology of 107 thyroid glands at necropsy (age range, 1-93 years) and showed that thyroid volume increased with age during childhood and adolescence, remained fairly constant in younger adults, and declined more slowly in older people related to a decrease in acinar size and not of acinar number.³⁸ Our results showed that thyroid gland volume decreased with age on MRI but did not significantly change with age on CT, although our youngest subject was only 10 years old. In our sample population,

we excluded subjects with CT or MRI findings of goiter, whereas the study of Dvorakova and coworkers likely included subjects with goiter related to iodine deficiency.

Age-associated histological findings of the thyroid gland have been documented, including a reduction in follicle size, degeneration and flattening of epithelial cells, increased interfollicular fibrosis, and varying lymphocytic infiltration.³⁹⁻⁴¹ Our data showed that the attenuation and maximum SUV of the thyroid gland did not significantly change with increasing age, which may be due to a balance between a decrease in acinar size along with a concomitant increase in lymphocytic and fibrous tissue infiltration. Similarly, El-Haddad and coworkers have shown that FDG uptake in the thyroid gland did not vary substantially with age.³ The MVP of the thyroid gland in our PET/CT subjects showed no significant change with increasing age.

Studies have been performed to evaluate thyroid function in the elderly. Mooradian and coworkers concluded that reduced thyroid hormone clearance with age explains the reduced daily replacement doses of thyroxine in hypothyroid elderly subjects.⁴² Chakraborti and coworkers showed that men older than the age of 60 had significantly lower T3 and thyroid-stimulating hormone levels and higher T4 levels compared with younger patients. They also found that a reduction in the basal and thyrotropin-releasing hormone induced a response of thyroid-stimulating hormone secretion with increasing age.⁴³ Habra and coworkers concluded that, in older people, serum total T4 and thyroxine-binding globulin levels remained stable, although total T3 levels were slightly diminished because of a lower combined production rate (by the thyroid gland and peripheral tissue) without a change in its clearance rate.⁴⁴ Mariotti and coworkers have found that aging is associated with an increased prevalence of thyroid autoantibodies and subclinical hypothyroidism. Thyroid autoantibodies were rare in centenarians and in other highly selected aged populations, but frequently observed in hospitalized elderly subjects, suggesting that thyroid autoimmune phenomena are not the consequence of the aging process itself but due to age-associated disease.⁴⁵

Tongue and Soft Palate

The tongue embryologically develops from the first pharyngeal arch. A study by Iskander and coworkers compared the neonatal and adult tongue to search for differences that would explain the functional specialization in neonatal tongues for suckling. The following observations were obtained from serial coronal sections of neonatal tongues with 3-dimensional reconstructions relative to the adult tongue: (1) there is considerably less fat and soft tissue; (2) there is a thinner mucosa; (3) there is relatively enlarged extrinsic musculature; (4) there is a less well-developed superior longitudinal muscle resulting in a flat dorsal surface; and (5) there are attachments between the extrinsic muscles and the transverse muscle group that have not been identified in the adult tongue.⁴⁶

A study by Temple and coworkers evaluated differential growth rates in the tongue and showed that the anterior

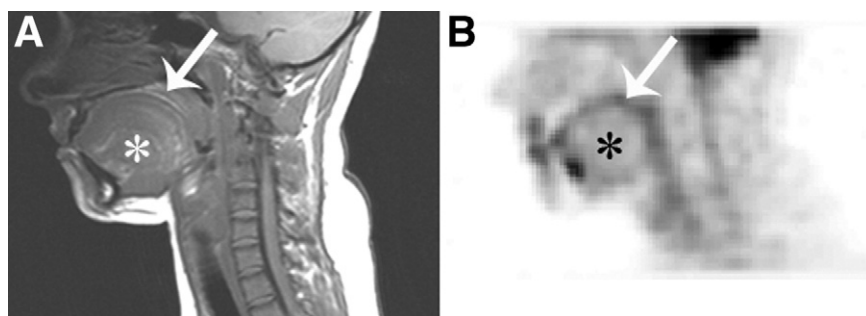


Figure 30 The tongue (*) and soft palate (arrow) seen here on a T1-weighted midsagittal MR image in a 28-year-old woman (A) and on a midsagittal FDG-PET image in an 18-year-old man (B). The maximum SUV of tongue was 2.2 and maximum SUV of soft palate was 2.5.

fungiform papillae-rich region of the tongue achieves adult size by 8 to 10 years of age, whereas the posterior region continues to grow until 15 to 16 years of age, without gender differences.⁴⁷ Rother and coworkers looked at the morphometric aging changes in the tongue and found that the mean cross-sectional area of the muscle fibers increases sharply during youth, remains at a high level into old age, and increases after the age of 70.⁴⁸ Ohnishi and coworkers reported that the tongue does not atrophy with increasing age based on area and perimeter measurements obtained from midsagittal MR images.⁴⁹ Similarly, we found that tongue volume measured on MRI did not significantly change with increasing age. However, we did observe a significant difference in tongue volume between males and females ($P < 0.00,001$) in our MRI group. The average tongue volume for males was 64.6 cm^3 (SD, 8.8; range, 51–88 cm^3), whereas for females it was 51.2 cm^3 (SD, 8.8; range, 36–80 cm^3).

Hirai and coworkers have shown that there are differences in tongue function with aging. Using ultrasonography, they concluded that upward and downward tongue movement rhythms in the elderly were more irregular than those of young adults and that velocities of upward and downward tongue movements were statistically decreased in the elderly ($P < 0.01$).⁵⁰ It has also been shown that tongue strength decreases with age.⁵¹ Studies that have measured tongue protrusion force and fatigability in patients have demonstrated that maximal tongue protrusion force decreases with age and tongue fatigability increases with age.^{52,53}

We also have observed a nonsignificant increase in the maximum SUV of the tongue with increasing age in our pediatric population. Unfortunately, we were unable to evaluate the change in maximum SUV of the tongue in adult subjects with increasing age based on measurements from PET/CT images due to beam hardening artifacts from dental amalgam that was present in 30 of 35 subjects. Dental amalgam produces defects on PET images as a result of excessive photon absorption, and can cause artifacts that mimic FDG uptake on PET/CT images.⁵⁴ However, El-Haddad and coworkers have shown that FDG uptake in the tongue and oral muscles did not vary substantially with age (Fig. 30).³ In addition, Nakamoto and coworkers reported that minimal FDG uptake is seen in the normal tongue on PET/CT (mean SUV of 1.39).²⁸

The effects of aging on taste perception, oral somatic sensation, and olfactory function have been evaluated. One study showed there was a significant age-related deterioration in taste sensation but not in oral somatic sensation.⁵⁵ Other studies have evaluated olfactory function with increasing age and have reported that olfactory function decreases with increasing age.^{56,57} It has been postulated that age-related loss of both taste perception and olfactory function have an additive effect in the decreased perception of taste in the elderly population.⁵⁵ This may not just reduce the pleasure and comfort of eating food but may increase the risk of nutritional and immune deficiencies as well as adherence to specific dietary regimens.⁵⁸

We have shown that soft-palate volume, as measured by MRI, significantly decreases with increasing age. Nakamoto and coworkers reported that intense FDG uptake usually was seen in the normal soft palate (mean SUV of 3.13; Fig. 30) and that mean soft palate SUV was slightly higher in men than in women on PET/CT.²⁸ Future research regarding the structure and metabolic activity of the soft palate will be pursued, as changes in soft palate morphology and function with age may have implications related to swallowing function.

Tonsils

Tonsils consist of aggregates of incompletely encapsulated lymphoid tissue. During development, the epithelial lining of the second pharyngeal pouch proliferates and forms buds that penetrate into the surrounding mesenchyme. The buds become infiltrated by mesodermal tissue, forming the primordium of the palatine tonsils, and are infiltrated by lymphatic tissue in the third to fifth months of gestation.⁵⁹ A similar process occurs for the adenoids and lingual tonsils.

Harada analyzed the age-related histopathological changes of the human palatine tonsils in 118 patients (age range from 6 months to 89 years) obtained from tonsillectomy or during autopsies and demonstrated the following: (1) the ratio of parenchymal area to the total tonsillar area decreased with age; (2) the average area of lymphoid follicles decreased with age; (3) the number of lymphoid follicles per unit area did not correlate with age, although the number remarkably decreased in patients older than the age of 70 years old; (4) the

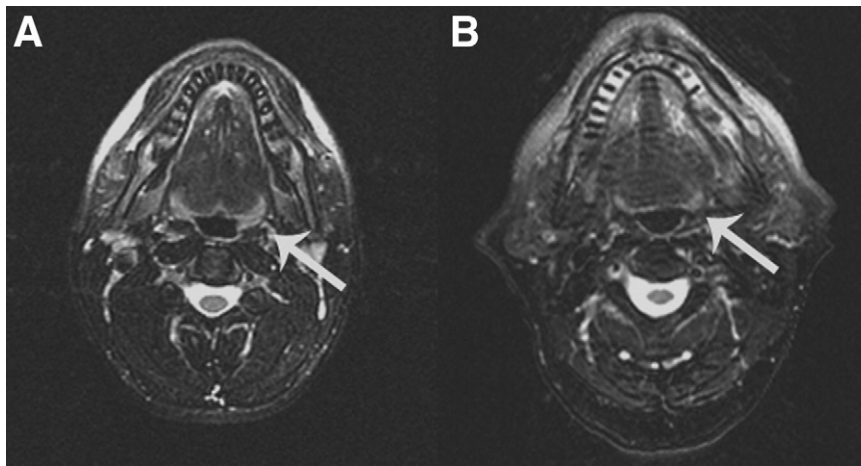


Figure 31 Axial T2-weighted MR images show the lingual tonsils (arrows) of an 18-year-old man (A) and of a 68-year-old man (B). The lingual tonsils are more prominent in (A).

lymphocyte infiltration number per unit area of crypt epithelium decreased with age; (5) the ratio of crypt area to the total area did not show a correlation with age although a tendency toward an increase with increasing age was seen; (6) the ratio of fibrous connective tissue area to total tonsillar area increased with age; (7) collagen fibers and elastic fibers had a tendency to increase with age; and (8) fatty degeneration began at about 25 years of age, was seen in most specimens from patients older than 35 years of age, and tended to increase with age.⁶⁰

Our results showed that there was no change in maximum SUV of the palatine tonsils with increasing age in our pediatric population, although Nakamoto and coworkers have reported a negative correlation between physiologic FDG uptake in the palatine tonsils with age.²⁸ In addition, we observed a significant negative correlation between lingual tonsil volume and increasing age (Fig. 31). We also noted that maximum SUVs of the lingual tonsils had a nonsignificant tendency to increase with age in our pediatric population. Furthermore, maximum SUVs of the adenoids significantly decreased with age in our pediatric population (Fig. 32). Nakamoto and coworkers reported that intense

FDG uptake was usually seen in the palatine tonsils (mean SUV of 3.48) and lingual tonsils (mean SUV, 3.11) on PET/CT.²⁸ El-Haddad and coworkers have shown that FDG uptake in the nasopharynx, larynx, and nose, as well as the eyelids and eye muscles did not vary substantially with age.³ Nakamoto and coworkers also reported that minimal FDG uptake was seen in the inferior concha (mean SUV, 1.56), and that FDG accumulation was variable in the vocal cords (mean SUV, 1.77) on PET/CT.²⁸

Study Limitations

Limitations of our study include its retrospective nature, its small study sample, the potential for sampling error in our measurements, and inability to obtain height and weight information in the majority of subjects. Furthermore, CT and MRI scans were performed on a variety of scanners using various scanning protocols, likely increasing the variability in measurements performed, and structure volume measurements were performed in different subjects who had either CT or MRI. Despite these limitations, we believe that our data provide useful information for those interested in studying changes in the head and neck with normal aging, and provide a basic methodological approach for future study of normal structural and functional changes in this region with aging.

Conclusion

CT, MRI, and PET are imaging modalities that may be used to quantitatively and qualitatively assess the structures of the head and neck and may be applied to the study of morphological and functional changes of these structures with aging. Such information can be used as a normative baseline to assess subjects of any age in the clinical setting who undergo head and neck imaging, and may be useful to aid investigators involved in aging-related research. In this article, we have reported quantitative preliminary data retrospectively obtained from CT, MRI, and PET imaging of the head and neck regarding changes in structural volume, attenuation, and metabolism with increasing age, and have reviewed the

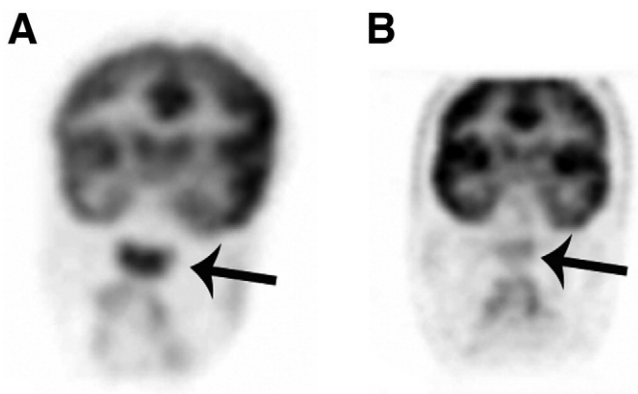


Figure 32 Coronal PET images of adenoids (arrows) in a 13-year-old boy (A), and an 18-year-old man (B). Note relatively decreased activity of adenoids in (B).

literature regarding reported changes in normal head and neck structure and function as well. We hope that some of these basic methodological approaches will be useful as a starting point for future prospective research regarding head and neck structural and functional changes with age.

References

- Vogl TJ, Dresel SH, Spath M, et al: Parotid gland: plain and gadolinium-enhanced MR imaging. *Radiology* 177:667-674, 1990
- Mees K, Vogl T, Kellermann O: Magnetic resonance tomography in tumors of the salivary glands—a diagnostic advantage? [in German]. *Laryngol Rhinol Otol (Stuttg)* 67:355-361, 1988
- El-Haddad G, Alavi A, Mavi A, et al: Normal variants in [18F]-fluorodeoxyglucose PET imaging. *Radiol Clin North Am* 42:1063-1081, 2004
- Silvers AR, Som PM: Salivary glands. *Radiol Clin North Am* 36:941-966, 1998
- Yousem DM, Kraut MA, Chalian AA: Major salivary gland imaging. *Radiology* 216:19-29, 2000
- Medbery R, Yousem DM, Needham MF, et al: Variation in parotid gland size, configuration, and anatomic relations. *Radiother Oncol* 54:87-89, 2000
- Scott J, Flower EA, Burns J: A quantitative study of histological changes in the human parotid gland occurring with adult age. *J Oral Pathol* 16:505-510, 1987
- Dong SZ: A quantitative morphologic study on age changes in the histologic structures of the human submandibular gland [in Chinese]. *Zhonghua Kou Qiang Yi Xue Za Zhi* 24:15-17, 62, 1989
- Kurashima C, Hirokawa K: Age-related increase of focal lymphocytic infiltration in the human submandibular glands. *J Oral Pathol* 15:172-178, 1986
- Azevedo LR, Damante JH, Lara VS, et al: Age-related changes in human sublingual glands: a post mortem study. *Arch Oral Biol* 50:565-574, 2005
- Martinez-Madrigal F, Micheau C: Histology of the major salivary glands. *Am J Surg Pathol* 13:879-899, 1989
- Dayan D, Vered M, Paz T, et al: Aging of human palatal salivary glands: A histomorphometric study. *Exp Gerontol* 35:85-93, 2000
- Waterhouse JP, Chisholm DM, Winter RB, et al: Replacement of functional parenchymal cells by fat and connective tissue in human submandibular salivary glands: an age-related change. *J Oral Pathol* 2:16-27, 1973
- Sumi M, Izumi M, Yonetsu K, et al: Sublingual gland: MR features of normal and diseased states. *AJR Am J Roentgenol* 172:717-722, 1999
- Ida M, Honda E: Age-dependent decrease in the computed tomographic numbers of parotid and submandibular salivary glands. *Dentomaxillofac Radiol* 18:31-35, 1989
- Ariji Y, Ariji E, Araki K, et al: Studies on the quantitative computed tomography of normal parotid and submandibular salivary glands. *Dentomaxillofac Radiol* 23:29-32, 1994
- Drummond JR, Newton JP, Abel RW: Tomographic measurements of age changes in the human parotid gland. *Gerodontology* 12:26-30, 1995
- Heo MS, Lee SC, Lee SS, et al: Quantitative analysis of normal major salivary glands using computed tomography. *Oral Surg Oral Med Oral Pathol Oral Radiol Endod* 92:240-244, 2001
- Yonetsu K, Yuasa K, Kanda S: Quantitative analysis of the submandibular gland using computed tomography. *Dentomaxillofac Radiol* 25:97-102, 1996
- Yeh CK, Johnson DA, Dodds MW: Impact of aging on human salivary gland function: A community-based study. *Aging (Milano)* 10:421-428, 1998
- Cowman RA, Frisch M, Lasseter CJ, et al: Effects of beta-adrenergic antagonists on salivary secretory function in individuals of different ages. *J Gerontol* 49:B208-214, 1994
- Ship JA, Nolan NE, Puckett SA: Longitudinal analysis of parotid and submandibular salivary flow rates in healthy, different-aged adults. *J Gerontol A Biol Sci Med Sci* 50:M285-289, 1995
- Jones RE, Ship JA: Major salivary gland flow rates in young and old, generally healthy African Americans and whites. *J Natl Med Assoc* 87:131-135, 1995
- Bourdiol P, Mioche L, Monier S: Effect of age on salivary flow obtained under feeding and non-feeding conditions. *J Oral Rehabil* 31:445-452, 2004
- Ship JA, Pillemer SR, Baum BJ: Xerostomia and the geriatric patient. *J Am Geriatr Soc* 50:535-543, 2002
- Ghezzi EM, Ship JA: Aging and secretory reserve capacity of major salivary glands. *J Dent Res* 82:844-848, 2003
- Stahl A, Dzewas B, Schwaiger M, et al: Excretion of FDG into saliva and its significance for PET imaging. *Nuklearmedizin* 41:214-216, 2002
- Nakamoto Y, Tatsumi M, Hammoud D, et al: Normal FDG distribution patterns in the head and neck: PET/CT evaluation. *Radiology* 234:879-885, 2005
- Gray H, Pick T, Howden R (eds): *The thyroid gland*, in *Gray's Anatomy, Book of Anatomy*. Philadelphia, PA, Running Press, 1974
- Jarlov AE, Hegedus L, Gjørup T, et al: Accuracy of the clinical assessment of thyroid size. *Dan Med Bull* 38:87-89, 1991
- Hermans R, Bouillon R, Laga K, et al: Estimation of thyroid gland volume by spiral computed tomography. *Eur Radiol* 7:214-216, 1997
- Nygaard B, Nygaard T, Court-Payen M, et al: Thyroid volume measured by ultrasonography and CT. *Acta Radiol* 43:269-274, 2002
- Yasuda S, Shohsu A, Ide M, et al: Diffuse F-18 FDG uptake in chronic thyroiditis. *Clin Nucl Med* 22:341, 1997
- Santiago JF, Jana S, El-Zeftawy H, et al: Increased F-18 fluorodeoxyglucose thyroidal uptake in Graves' disease. *Clin Nucl Med* 24:714-715, 1999
- Cohen MS, Arslan N, Dehdashti F, et al: Risk of malignancy in thyroid incidentalomas identified by fluorodeoxyglucose-positron emission tomography. *Surgery* 130:941-946, 2001
- Yi JG, Marom EM, Munden RF, et al: Focal uptake of fluorodeoxyglucose by the thyroid in patients undergoing initial disease staging with combined PET/CT for non-small cell lung cancer. *Radiology* 236:271-275, 2005
- Dvorakova M, Bilek R, Cerovska J, et al: The volumes of the thyroid gland in adults aged 18-65 years in the Czech Republic—determination of the norms [in Czech]. *Vnitř Lek* 52:57-63, 2006
- Brown RA, Al-Moussa M, Beck J: Histometry of normal thyroid in man. *J Clin Pathol* 39:475-482, 1986
- Andrew W, Andrew WV: Senile involution of the thyroid gland. *Am J Pathol* 18:849-863, 1942
- Mustacchi PO, Lowenhaupt E: Senile changes in the histologic structure of the thyroid gland. *Geriatrics* 5:268-273, 1950
- Pittman JA Jr: The thyroid and aging. *J Am Geriatr Soc* 10:10-21, 1962
- Mooradian AD: Normal age-related changes in thyroid hormone economy. *Clin Geriatr Med* 11:159-169, 1995
- Chakraborti S, Chakraborti T, Mandal M, et al: Hypothalamic-pituitary-thyroid axis status of humans during development of ageing process. *Clin Chim Acta* 288:137-145, 1999
- Habra M, Sarlis NJ: Thyroid and aging. *Rev Endocr Metab Disord* 6:145-154, 2005
- Mariotti S, Franceschi C, Cossarizza A, et al: The aging thyroid. *Endocr Rev* 16:686-715, 1995
- Iskander A, Sanders I: Morphological comparison between neonatal and adult human tongues. *Ann Otol Rhinol Laryngol* 112:768-776, 2003
- Temple EC, Hutchinson I, Laing DG, et al: Taste development: differential growth rates of tongue regions in humans. *Brain Res Dev Brain Res* 135:65-70, 2002
- Rother P, Wohlgemuth B, Wolff W, et al: Morphometrically observable aging changes in the human tongue. *Ann Anat* 184:159-164, 2002
- Ohnishi A, Oishi T, Murai Y, et al: Quantitative evaluation of tongue atrophy on midsagittal magnetic resonance images (MRIs) [in Japanese]. *Rinsho Shinkeigaku* 32:317-320, 1992
- Hirai T, Tanaka O, Koshino H, et al: Aging and tongue skill. Ultrasound (motion-mode) evaluation [in Japanese]. *Nihon Hotetsu Shika Gakkai Zasshi* 33:457-465, 1989

51. Crow HC, Ship JA: Tongue strength and endurance in different aged individuals. *J Gerontol A Biol Sci Med Sci* 51:M247-250, 1996
52. Mortimore IL, Fiddes P, Stephens S, et al: Tongue protrusion force and fatigability in male and female subjects. *Eur Respir J* 14:191-195, 1999
53. Mortimore IL, Bennett SP, Douglas NJ: Tongue protrusion strength and fatigability: relationship to apnoea/hypopnoea index and age. *J Sleep Res* 9:389-393, 2000
54. Goerres GW, Von Schulthess GK, Hany TF: Positron emission tomography and PET CT of the head and neck: FDG uptake in normal anatomy, in benign lesions, and in changes resulting from treatment. *AJR Am J Roentgenol* 179:1337-1343, 2002
55. Fukunaga A, Uematsu H, Sugimoto K: Influences of aging on taste perception and oral somatic sensation. *J Gerontol A Biol Sci Med Sci* 60:109-113, 2005
56. Doty RL, Shaman P, Applebaum SL, et al: Smell identification ability: Changes with age. *Science* 226:1441-1443, 1984
57. Cain WS, Stevens JC: Uniformity of olfactory loss in aging. *Ann N Y Acad Sci* 561:29-38, 1989
58. Schiffman SS: Taste and smell losses in normal aging and disease. *JAMA* 278:1357-1362, 1997
59. Langman J: Head and neck, in Langman J (ed): *Medical Embryology*. Baltimore, MD, Williams and Wilkins, 1981, p 275
60. Harada K: The histopathological study of human palatine tonsils—especially age changes [in Japanese]. *Nippon Jibiinkoka Gakkai Kaiho* 92:1049-1064, 1989